



Application of the direct strength method to functionally-graded-material-sheathed cold-formed steel beam channel members under non-uniform elevated temperature

Elias Y. Ali¹, Yared Shifferaw²

Abstract

The objective of this paper is to examine the application of the Direct Strength Method (DSM) to determine the strength of cold-formed steel (CFS) beam channel members under non-uniform elevated temperature using Functionally Graded Material (FGM) as a thermal barrier. Functionally graded materials are advanced materials characterized by non-homogenous material system with gradual gradation of material property within a given dimension. The composition of the FGM sheathing is defined by using the volume fractions of the constituent materials distributed across the thickness direction. When a cold-formed steel member is subjected to fire (or a thermal gradient) on one side of the panel, material properties change – but this change happens around the cross-section and along the length creating a member which is potentially non-uniform and unsymmetrical in its response even if the apparent geometry is uniform and symmetric. The heat transfer analysis is completed using ABAQUS to obtain the time-dependent temperature distribution on the CFS cross-sections. The influence of sheathing material on the response of the members is compared with the strength of same sections with gypsum board as a thermal barrier. DSM strength formulations are examined following stability analyses performed to characterize how local, distortional, and global buckling of the members evolve under elevated temperature, in which mechanical properties are considered temperature dependent.

1. Introduction

Fire safety and the behavior of cold-formed steel (CFS) structures under elevated temperature is gaining high interest due to the increasing incidents of major fires in building compartments and infrastructures. Cold-formed steel (CFS) commonly used in low to mid-rise structures, in residential, industrial and commercial buildings as framing, partition walls, and exterior walls and as load-bearing structural components in floor and roofing systems. This growing interest in thin-walled structural members in general and cold-formed steel in particular is due to their unique advantage of high strength to weight ratio. However, under elevated temperature, steel would quickly heats up resulting in a rapid reduction in its mechanical properties, particularly the yield strength and stiffness.

¹ PhD Candidate, Drexel University, <eya24@drexel.edu>

² Assistant Professor, Drexel University, <yaredshi@drexel.edu>

These reductions in mechanical properties have been investigated by researchers both experimentally and numerically (Kankanamge and Mahendran 2011). It is found that the reductions in strength and stiffness are even more significant in cold-formed steels. Cold-formed steel members that are commonly used in structural wall and floor systems are protected by materials such as gypsum board, with or without insulation. However, the efficiency of gypsum board is dependent on its thickness, availability of insulation and is only effective to prevent spread of temperature until the small water contained in it is driven off (Rahmanian 2011). Functionally Graded Materials (FGMs) are advanced materials characterized by non-homogenous material system with gradual gradation of material property within a given dimension. This gradation is achieved by either combining two or more materials using volume-fraction or by treating a single material chemically to change its initial properties. The functionally graded composite material will then have a unique and different material property from the individual constituent materials while preserving their individual benefits. The concept of FGM first originated in Japan in 1984 during the hypersonic space plane project as a thermal barrier to resist high temperature gradient with outside temperature of 2000K and an inside temperature of 1000K across a thickness of less than 10 mm for space shuttles (Rasheedat M. Mahamood 2012).

The application of functionally graded materials (FGMs) as thermal barrier has gained more interest among researchers recently leading to extensive research in the development and manufacturing of FGMs. Numerical analysis of steady state heat conduction in composite FGMs has been investigated by (Liviu Marin 2010). A finite element formulation of a coupled thermo-mechanical problem in functionally graded metal/ceramic plates as studied by (Burlayenko et al. 2017). The theoretical framework of the finite element method (FEM) applied to the development of a functionally graded two-dimensional plane strain finite element was considered. Advanced computational method for transient heat conduction analysis in continuously nonhomogeneous functionally graded materials (FGM) was proposed by (Sladek et al. 2003). The method was based on the local boundary integral equations with moving least square approximation of the temperature and heat flux. Transient temperature response of functionally graded materials subjected to pulse or stepwise heating at the front surface was evaluated by (Ishiguro et al. 1993). A feasibility study with simple and economical methods on production of FGM and their thermal analysis for thermal barrier specifically for hypersonic structures was conducted and presented in the report by (Sook-Ying et al. 2007). For potential application of ceramics as a thermal barrier coating (TBC) in a functionally graded composite, properties of some of ceramic materials were summarized by (Cao et al. 2004).

Though FGM is intensively exploited for thermo-mechanical problems, their applicability for fire protection in thin-walled structural systems is rare or unavailable to date. Thus, the main goal of this paper would be to examine the performance of CFS beams under fire protected by FGM thermal barrier.

2. Functionally graded material (FGM) thermal barrier

In this study, it is assumed that the FGM barrier has 12.5mm (0.5 in) thickness with ten layers. Each layer is assumed to be composed of an isotropic and homogenous material based on the volume fraction defined using the power law. Fire exposed face of the FGM is considered to be

ceramic (100% ZrO₂) which gradually changes to Titanium alloy (100% Ti-6Al-4V) in the inner face of the board as shown in Fig. 1.

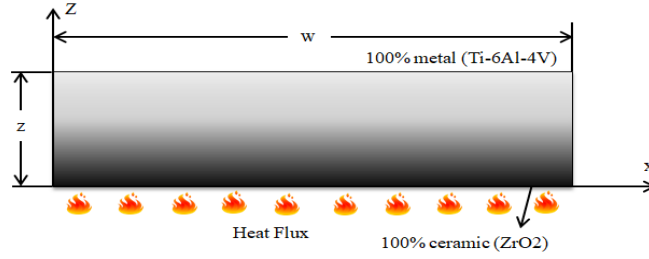


Figure 1: Composition of FGM for thermal barrier

For better understanding of the behavior of functionally graded materials in high temperature environment, a reliable material property under thermo-mechanical condition is essential for predicting the heat transfer behavior in the FGM. The constitutive material property which varies through the thickness of the thermal barrier is expressed using volume fraction variation, which can be described using the power law function, exponential function, or sigmoid function. The volume fraction of the metal phase suggested by (Burlayenko et al. 2017) using a power function law is given in Eq. 1.

$$V_m = \left(\frac{z}{h}\right)^n \quad (1)$$

Where h is thickness of the FGM sheathing and n is the volume fraction component. The volume fraction of the ceramic phase is then calculated as $V_c = 1 - V_m$. Using the above power law function, the FGM is ceramic rich when the parameter $n > 1$ and metal rich when $n < 1$.

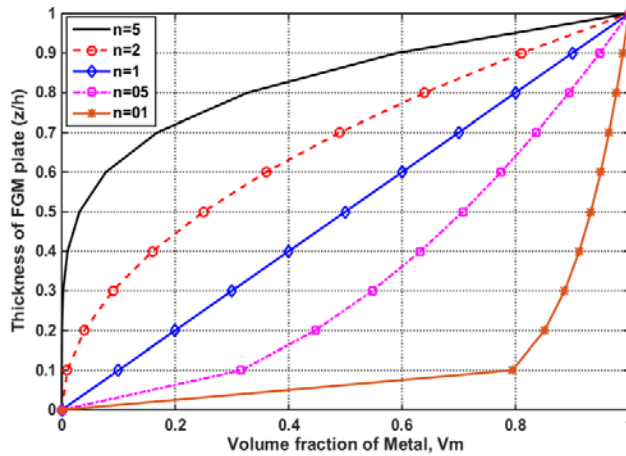


Figure 2: Variation of volume fraction through FGM for different power-law index (n-value)

Once the local volume fraction is defined, the functional relation of material properties at any point across the thickness of the thermal barrier can be expressed according to the general rule of mixture given by Eqs. (2-5).

$$E(z) = E_c \left\{ \frac{E_c + (E_m - E_c)V_m^{2/3}}{E_c + (E_m - E_c)V_m^{2/3} - V_m} \right\} \quad (2)$$

$$\rho(z) = \rho_m V_m + \rho_c V_c \quad (3)$$

$$k(z) = k_c \left\{ \frac{1 + 3(k_m - k_c)V_m}{3k_c + (k_m - k_c)V_c} \right\} \quad (4)$$

$$c(z) = \frac{c_m \rho_m V_m + c_c \rho_c V_c}{\rho_m V_m + \rho_c V_c} \quad (5)$$

Where E , ρ , k and c are Young's modulus, mass density, thermal conductivity and specific heat respectively, which are all spatially dependent functions.

3. Thermal analysis

Evaluating the non-uniform temperature distribution in the CFS channel cross-section, which is protected by FGM board, requires heat transfer analysis which was conducted using the finite element program ABAQUS. There are two approaches to perform the heat transfer analysis in an FGM board protected cold-formed member: (i) time-dependent and (ii) both time and space dependent. The time-dependent analysis is a 2-D heat transfer problem considering uniform temperature along longitudinal member length but which would vary along the cross-section with time. In time and space dependent analysis, temperature distribution is not uniform and may vary both across and along the longitudinal member with both time and location. Fig. 3 shows the fire temperature used in the heat transfer analysis defined using Eq. 6 of the ISO834 standard fire and the fire exposure of the FGM-sheathed CFS channel member considered in the paper.

$$T = T_a + 345 \log(8t / 60 + 1) \quad (6)$$

Where: $T_a=20^\circ\text{C}$ is the ambient temperature and t is time in seconds.

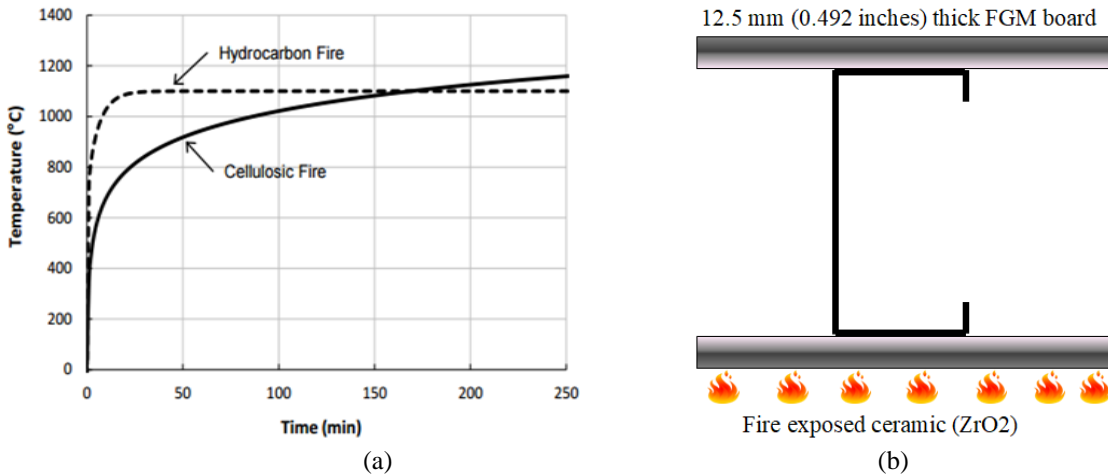


Figure 3: Fire load and geometry of the panel (a) ISO834 standard fire (b) CFS channel section protected by FGM board

Material properties used in the heat transfer analysis are density, thermal conductivity and specific heat for both steel and FGM boards which vary with temperature. In the work presented herein the material properties adopted for thermal analysis for steel and gypsum (Feng et al. 2003) and for ceramic and metal FGM components (Nemat-Alla et al. 2009) as given in Table 1.

Table 1: Material properties used in heat transfer analysis

Material	Density (kg/m)	Thermal conductivity	Specific heat
Steel	7850	$54 - 3.33 * 10^{-2} (T)$ (20 °C ≤ T ≤ 800 °C) (W/m °C)	$425 + 7.73 * 10^{-1} (T) - 1.69 * 10^{-3} (T^2) + 2.22 * 10^{-6} (T^3)$ (20 °C ≤ T < 600 °C) (J/kg °C)
Gypsum	727	0.2 at 10 °C 0.218 at 150 °C 0.319 at 1200 °C	925.04 at 10 °C 941 at 95 °C 953 at 1 ⁵⁰ C
Ceramic (ZrO2)	3658	$1.71 + 0.21 * 10^{-3} (T) + 0.116 * 10^{-6} (T^2)$ (W/mK)	$274 + 7.95 * 10^{-1} (T) - 6.19 * 10^{-4} (T^2) + 1.71 * 10^{-7} (T^3)$ (J/KgK)
Metal (Ti6Al4V)	4420	$1.1 + 0.017 (T)$ (W/mK)	$350 + 8.78 * 10^{-1} (T) - 9.74 * 10^{-4} (T^2) + 4.43 * 10^{-7} (T^3)$ (J/KgK)

The thermal boundary conditions considered during the heat transfer analysis are convection and radiation for both fire exposed and ambient sides. These interaction properties are defined by convection surface film coefficient of 25W/m²K and 10W/m²K for exposed side and ambient side respectively, radiation film coefficient of 25W/m²K for fire exposed side, and emissivity of 0.3 and 0.8 for fire exposed and ambient sides respectively.

Fig. 4 shows the temperature profile for channel section 400S200-54 (web height=4 in., flange width =2 in. and design thickness=0.0556 in.) after full fire time. It can be observed that the temperature in the web elements of the CFS section is not uniform with the highest temperature at parts closer to the fire exposed side and gradually tends to attain smaller temperature at the unexposed surface. Temperature in the unexposed flange and lip remains relatively low even after 120 minute of fire exposure, compared to the fire exposed flange and lip.

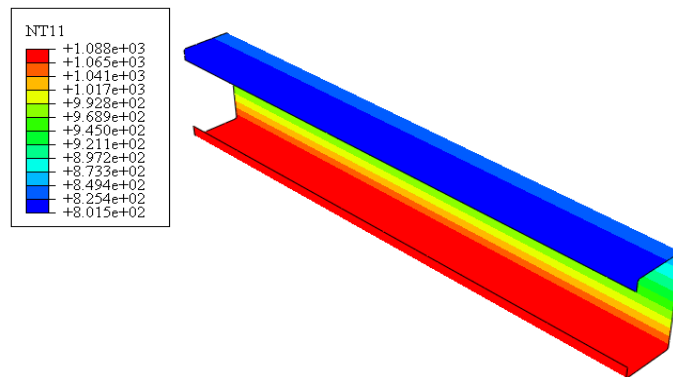


Figure 4: Temperature distribution on CFS section after heat transfer analysis

The effect of sheathing material and thickness on the temperature distribution at fire exposed flange and mid-web of the channel section is presented in Fig. 5. It can be observed that the maximum temperature at fire exposed flange and mid-web for both gypsum and FGM sheathing exhibit relatively similar temperature distribution. Slight temperature difference is observed up to 120 seconds fire period. The CFS would eventually exhibit same temperature distribution. The reason for this is the thickness (0.5 inch) used for fire protection is very thin that it would only protect the fire spread only for few minutes in both sheathing materials.

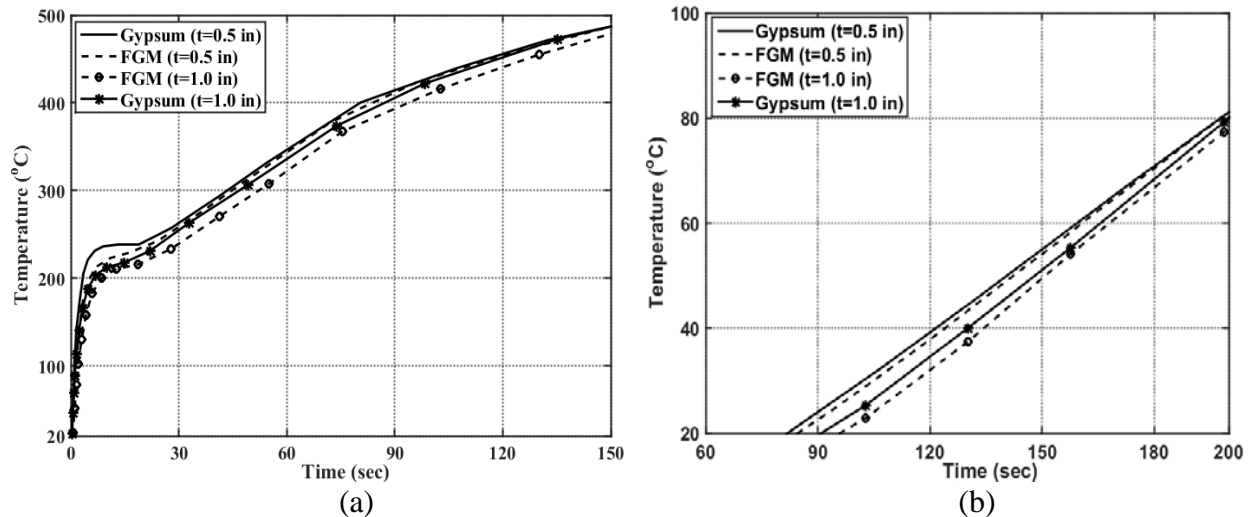


Figure 5: Temperature distribution comparisons on CFS (a) Fire exposed flange (b) mid-web

4. Stability of FGM-sheathed CFS beam under elevated temperature

Past researchers such as (Alfawakhiri 2002, Kankanamge 2010, Shahbazian and Wang 2011) have investigated the buckling behavior and resistance of cold formed steel members at uniform elevated temperature. However, there are only limited studies on the buckling behavior and responses of cold-formed steel beams under pure bending with non-uniform temperature distribution. During fire, the temperature distribution along the section is usually assumed to be uniform, for analytical simplicity, both across the section and along the member length. Thus, the buckling behavior is analyzed based on uniform reduced material properties. However, in real fire scenario, the temperature distribution in a steel section is generally not uniform. This is especially true when cold-formed steel structural member is exposed to fire only on one side. Thus, the temperature-dependent material properties, yield strength, elastic modulus and coefficient of thermal expansion, would vary with in the section and along the member. This was investigated by (Cheng et al. 2015) after several experimental tests. This phenomenon would make the buckling behavior and analysis more complicated than the commonly practiced analysis approach.

For the FE analyses, a simply supported member is considered; where at both ends of the beam lateral (u_2), transverse (u_3) and twisting in the minor axis (u_{R1}) are restrained. Four nodes S4R5 shell elements and a global mesh size of 0.1 inch were used in both elastic and collapse analyses. The elastic buckling analysis of the 400S200-54 section considered in this paper shows that there is a reduction in critical buckling moments with increased fire in both uniform (Fig. 6) and non-uniform temperature distribution (Fig.7). These reductions exhibit the same pattern as the

reduction in steel material properties, mainly the modulus of elasticity, as shown in Table 2. It has a small or gradual reduction until the maximum flange temperature reaches 300°C and follows with steep reduction in buckling moment up to 600°C, then starts to exhibit a gradual change from 600°C-800°C. The critical buckling moment curve for section under uniform temperature also exhibits three buckling modes: local, distortional and global buckling. Local buckling mode is predominant for the half wave length of up to 5 inches and the distortional buckling mode is predominant at a half wave length of 12 inches to 60 inches.

For the non-uniform temperature distribution case, the critical buckling moment curve exhibits mainly local and distortional buckling modes. Local buckling mode occurs for the half wave length of up to 10 inches while distortional buckling mode is predominant at a half wave length of 12 inch and above. The non-uniform temperature distribution also resulted in higher critical buckling moment than the uniform temperature cases. The reason for such behavior can be explained by the relatively lower temperature across the section which in turn results in higher rigidity in both compression flanges and web.

Table 2: Reduction factors of mechanical properties of CFS at elevated temperature (Kankanamge 2010)

Temperature (°C)	20	100	200	300	400	500	600	700	800
$k_{yT}=(f_{y,T}/f_{y,20})$	1	0.9995	0.9903	0.9519	0.694	0.3906	0.1109	0.07	0.03
$k_{ET}=(E_T/E_{20})$	1	0.9332	0.8497	0.7151	0.5801	0.4451	0.3101	0.1751	0.0401

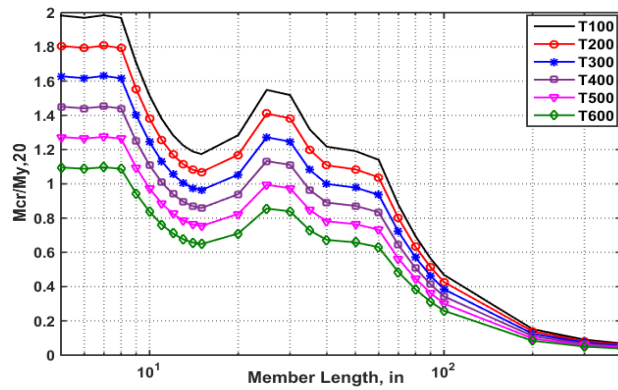


Figure 6: Normalized critical buckling moment under uniform temperature distribution

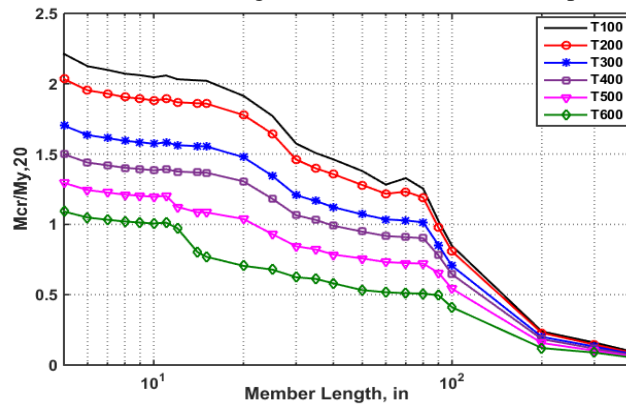


Figure 7: Normalized critical buckling moment under non-uniform temperature distribution

5. Collapse analysis of FGM-sheathed CFS beam under non-uniform temperature

Finite element collapse analysis of the FGM-sheathed CFS beam under elevated temperature is considered with the true stress-strain material model adopted in ABAQUS. Thus, to observe the collapse behavior, an elastic-perfect plastic or strain hardening material modeling can be considered. In the elastic-perfect plastic material model the yield stress on the material remains unchanged with increase in plastic strain, whereas in isotropic strain hardening, for example, strain-hardening occurs with the stress varying as a function of the plastic strain. Based on the experimental result by (Kankanamge 2010) higher grade cold-formed steels shows isotropic hardening behavior at both ambient and elevated temperatures, whereas, low-grade CFS exhibits a well-defined yield point at a temperature range below 500°C. In this non-linear collapse analysis, an elastic-perfect plastic material model as shown in Fig. 8 is used.

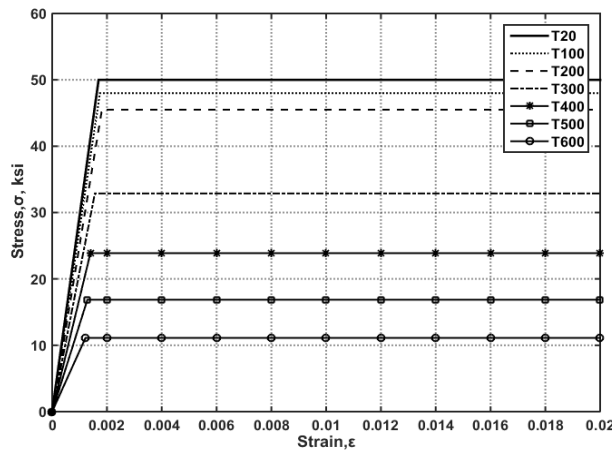


Figure 8: Stress-strain relationship of CFS at elevated temperatures

The non-linear collapse analysis is performed on members without imperfection using RIKS algorithm in ABAQUS. Predefined non-uniform temperature is imported from the heat transfer output files for each time step. The critical distortional buckling moment from elastic analysis is then applied at the simply supported end for each time step. FE collapse mode under non-uniform elevated temperature distribution for considered section is illustrated in Fig. 9.

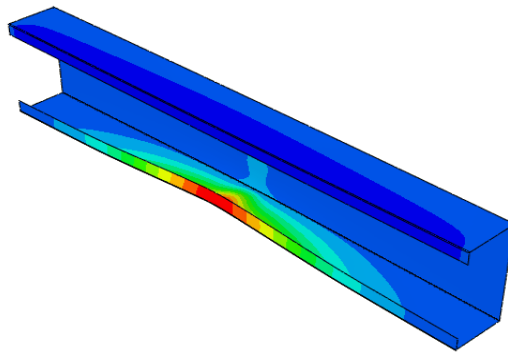


Figure 9: Collapse mode for section 400S200-54 under elevated temperature

The effect of sheathing material on collapse moment for moderate temperature ranges (100°C-200°C) is shown in Fig. 10. It is observed that CFS sheathed with FGM shows a relatively higher

moment capacity than the one with gypsum when a temperature at any point in the fire exposed flange reaches 300°C. This section capacity difference would gradually be insignificant when temperature exceeds 400°C. Once the fire temperature on fire exposed flange exceeds 400°C, temperature distribution and section capacity are mainly dependent only on the thermal material properties of the steel.

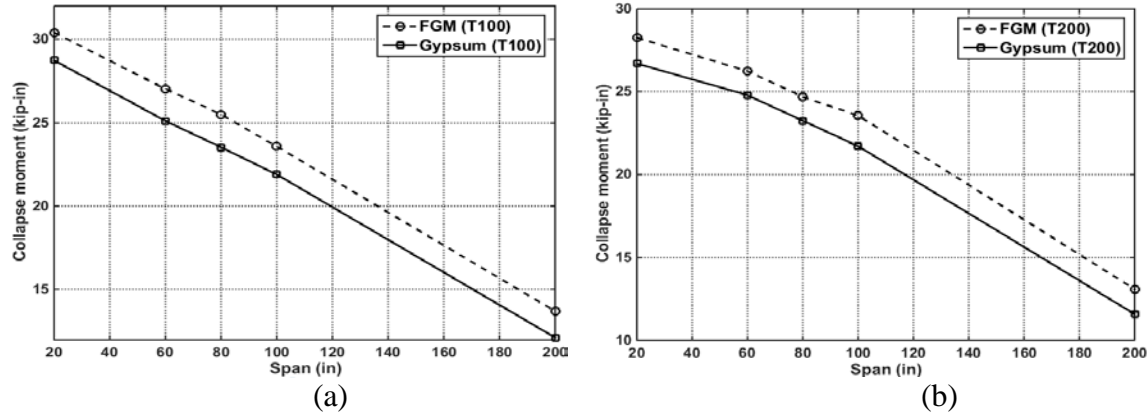


Figure 10: Section moment capacity under non-uniform temperature (a) T=100°C and (b) T=200°C

6. Direct Strength Method examination of FGM-sheathed CFS beam under elevated temperature

To calculate the load carrying capacity of CFS members, the Effective Width Method (EWM) has been used. However, using EWM to determine the effective section is very tedious and time consuming for cross-section with intermediate stiffeners and very long iterations are required to determine member strength, with the impact of elevated temperature greatly exacerbating prediction complexities. To overcome such issues in EWM, Schafer (2006) developed the Direct Strength Method (DSM) which is based on the gross cross-section of the CFS member. For any cross-section of a member, it is assumed the design strength could be determined by using elastic critical buckling load and the yield strength of the cross-section.

DSM design formulations provided in AISI (2016) for calculating the nominal flexural strength of members are M_{ne} , M_{nl} and M_{nd} representing lateral-torsional, local and distortional buckling respectively and are given in Eqs. (7-9). The moment resistance for a CFS member under ambient temperature is the minimum of M_{ne} , M_{nl} and M_{nd} .

$$M_{ne} = \begin{cases} M_y & M_{cre} > 2.78M_y \\ \frac{10}{9}M_y \left(1 - \frac{10M_y}{36M_{cre}}\right) & 0.56M_y \leq M_{cre} < 2.78M_y \\ M_{cre} & M_{cre} < 0.56M_y \end{cases} \quad (7)$$

$$M_{nl} = \begin{cases} M_{ne} & \lambda_1 \leq 0.776 \\ \left(1 - 0.15 \left(\frac{M_{crl}}{M_{ne}}\right)^{0.4}\right) \left(\frac{M_{crl}}{M_{ne}}\right)^{0.4} M_{ne} & \lambda_1 > 0.776 \end{cases} \quad (8)$$

$$M_{nd} = \begin{cases} M_y & \lambda_d \leq 0.673 \\ \left(1 - 0.22 \left(\frac{M_{crd}}{M_y}\right)^{0.5}\right) \left(\frac{M_{crd}}{M_y}\right)^{0.5} M_y & \lambda_d > 0.673 \end{cases} \quad (9)$$

Where

M_y is the yield moment of the beam and M_{cre} is the elastic critical lateral-torsional buckling moment

$\lambda_l = \sqrt{M_{ne} / M_{crl}}$ and M_{crl} is the elastic critical local buckling moment

$\lambda_d = \sqrt{M_y / M_{crd}}$ and M_{crd} is the elastic critical distortional buckling moment

From Fig. 11 it can be observed that the FE collapse analyses using uniform temperature distribution and DSM Eq. 9 for distortional section capacity are in good agreement for all temperature ranges considered in the collapse analysis. Up to 6.5% difference is observed for beam length 200 inches at a temperature of 400°C (Table 3). This difference is caused due to a combination of distortional buckling and lateral distortional buckling modes at such beam length. In all the temperature ranges, the DSM equation gives lower (conservative) section capacity than the FE collapse analysis especially for beam slenderness ranging from 1 to 2.5.

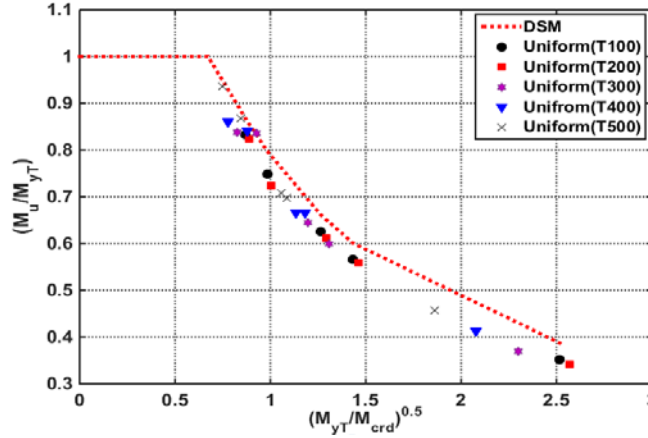


Figure 11: Distortional buckling mode strength prediction under uniform elevated temperature

Table 3: Section moment capacity under uniform elevated temperature

Span(in)	Moment (in-kip)	Maximum Temperature(°C)						
		20	100	200	300	400	500	600
20	FE collapse	28.9	27.63	25.92	19.05	14.2	10.91	7.21
	DSM	29.92	28.45	26.61	20.21	15.19	10.99	7.36
	% diff	3.4	2.88	2.611	5.76	6.55	0.9	2.05
60	FE collapse	25.43	24.81	22.75	18.98	13.87	10.1	6.54
	DSM	27.57	26.19	24.47	18.66	14.07	10.21	6.85
	% diff	7.76	5.33	7.06	1.68	1.45	1.11	4.49
80	FE collapse	21.65	20.72	19.21	14.63	10.98	8.13	5.64

	DSM	22.83	21.65	20.2	15.5	11.74	8.56	5.75
	% diff	5.15	4.27	4.91	5.61	6.45	4.98	1.84
100	FE collapse	19.581	18.77	17.56	13.63	10.98	8.25	5.56
	DSM	20.77	19.61	18.28	14.45	11.37	8.72	5.61
	% diff	5.75	4.29	3.95	5.64	3.44	5.33	0.99
200	FE collapse	12.54	11.68	10.74	8.4	6.83	5.33	4.01
	DSM	13.38	12.03	11.2	8.94	7.11	5.52	4.07
	% diff	6.31	2.92	4.06	6.05	3.91	3.35	1.67

The FE analysis results using a non-uniform temperature distribution and DSM Eq. 9 for distortional buckling capacity are observed to be in good agreement only in few cases. There is a significant difference for moderate temperature ranges (up to 400°C) as shown in Fig. 12 and Table 4. Thus, it is recommended to modify the original DSM equation to incorporate the non-uniform temperature effect on section stability and strength.

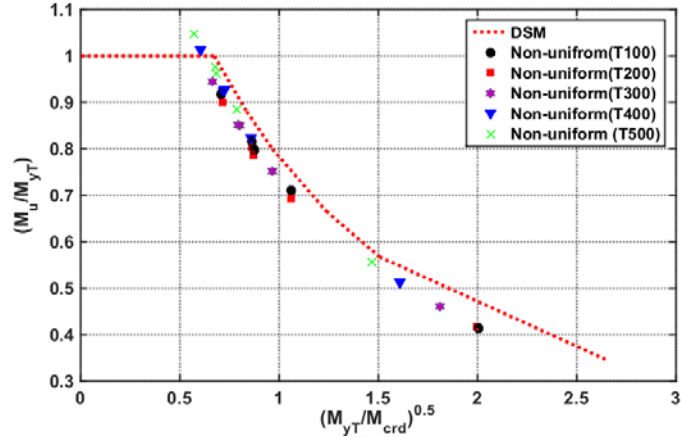


Figure 12: Distortional buckling mode strength prediction under non-uniform elevated temperature

Table 4: Section moment capacity under non-uniform elevated temperature

Span(in)	Moment (in-kip)	Maximum Temperature(°C)					
		100	200	300	400	500	600
20	FE collapse	30.407	28.248	21.436	16.692	12.198	7.552
	DSM	32.28	30.43	22.82	17.36	12.55	7.673
	% diff	5.802	7.171	6.063	3.846	2.806	1.583
60	FE collapse	27.03	25.238	19.319	15.208	11.377	7.562
	DSM	28.58	27.112	20.64	15.89	11.6	7.673
	% diff	5.423	6.914	6.398	4.293	1.922	1.447
80	FE collapse	26.426	24.686	19.283	15.269	11.212	7.546
	DSM	28.37	26.91	20.51	15.82	11.56	7.673
	% diff	6.853	8.266	5.984	3.486	3.01	1.654
100	FE collapse	23.557	21.775	17.042	13.578	10.308	7.092
	DSM	24.71	23.48	18.16	14.27	10.65	7.31

	% diff	4.667	7.263	6.155	4.85	3.208	2.982
	FE collapse	13.704	13.088	10.445	8.448	6.485	4.592
200	DSM	14.73	14.01	11.01	8.84	6.75	4.74
	% diff	6.968	6.581	5.136	4.431	3.919	3.118

7. Conclusions and future research

Numerical heat transfer, stability and collapse analyses on the potential application of functionally graded materials (FGM) as a sheathing material for fire protection and the application of the Direct Strength Method (DSM) to cold-formed steel channel section beam members protected by functionally graded material under elevated temperatures were undertaken. It was observed that functionally graded material show a relatively better performance to prevent the spread of fire temperature to CFS up to 400°C (120 seconds of fire exposure) and higher section moment capacity at these temperature ranges compared with the same section protected by gypsum. This performance can be improved by increasing the thickness of the sheathing and including insulation. The comparison on application of DSM for uniform and non-uniform temperature distribution on CFS confirm that the DSM distortional strength and FE results are in relatively good agreement for a uniform temperature application, whereas for a non-uniform temperature application, there is significant difference between the two capacities and modification on the DSM distortional buckling equation is needed.

The results presented herein considered a simply supported lipped channel member in pure bending loading. In order to properly examine the behavior of functionally-graded-material sheathed cold-formed steel members and strength prediction through DSM formulations more accurately, future research effort would need to extend the current observations to include separation of stability modes involving comprehensive parametric study that would account for the effect of FGM and CFS geometry, material models, loading and boundary conditions under elevated temperature.

References

- AISI (2016). North American Specification for the Design of Cold-Formed Steel Structural Members
- Alfawakhiri, F. (2002). Behaviour of cold-formed-steel-framed walls and floors in standard fire resistance tests. Ph.D., Carleton University.
- Burlayenko, V. N., H. Altenbach, T. Sadowski, S. D. Dimitrova and A. Bhaskar (2017). "Modelling functionally graded materials in heat transfer and thermal stress analysis by means of graded finite elements." *Applied Mathematical Modelling* **45**: 422-438.
- Cao, X. Q., R. Vassen and D. Stoeber (2004). "Ceramic materials for thermal barrier coatings." *Journal of the European Ceramic Society* **24**(1): 1-10.
- Cheng, S., L.-y. Li and B. Kim (2015). "Buckling analysis of cold-formed steel channel-section beams at elevated temperatures." *Journal of Constructional Steel Research* **104**: 74-80.
- Feng, M., Y. C. Wang and J. M. Davies (2003). "Thermal performance of cold-formed thin-walled steel panel systems in fire." *Fire Safety Journal* **38**(4): 365-394.
- Ishiguro, T., A. Makino, N. A. and N. Noda (1993). "Transient Temperature Response in Functionally Gradient Materials." *International Journal of Thermophysics* **14**(1).
- Kankanamge, N. D. (2010). Structural Behaviour and Design of Cold-formed Steel Beams at Elevated Temperatures, Queensland University of Technology.
- Kankanamge, N. D. (2010). Structural Behaviour and Design of Cold-Formed Steel under Elevated Temperatures. Ph.D., Queensland University of Technology.
- Kankanamge, N. D. and M. Mahendran (2011). "Mechanical properties of cold-formed steels at elevated temperatures." *Thin-Walled Structures* **49**(1): 26-44.

- Liviu Marin, D. L. (2010) "Heat transfer in functionally graded materials using the method of fundamental solutions."
- Nemat-Alla, M., K. I. E. Ahmed and I. Hassab-Allah (2009). "Elastic-plastic analysis of two-dimensional functionally graded materials under thermal loading." *International Journal of Solids and Structures* **46**(14-15): 2774-2786.
- Rahmanian, I. (2011). Thermal and mechanical properties of gypsum boards and their influence on fire resistance of gypsum based systems. PhD, University of Manchester.
- Rasheedat M. Mahamood, E. T. A. (2012). "Functionally Graded Material. An Overview." *Proceedings of the World Congress on Engineering 2012 Vol III*
- Schafer, B. W. (2006). Review: The Direct Strength Method of Cold-Formed Steel Member Design. *STABILITY AND DUCTILITY OF STEEL STRUCTURES*. Lisbon, Portugal.
- Shahbazian, A. and Y. C. Wang (2011). "Calculating the global buckling resistance of thin-walled steel members with uniform and non-uniform elevated temperatures under axial compression." *Thin-Walled Structures* **49**(11): 1415-1428.
- Sladek, J., V. Sladek and C. Zhang (2003). "Transient heat conduction analysis in functionally graded materials by the meshless local boundary integral equation method." *Computational Materials Science* **28**(3-4): 494-504.
- Sook-Ying, H., A. Kotousov, P. Nguyen and H. Tsukamoto (2007). *FGM (Functionally Graded Material) Thermal barrier Coatings for Hypersonic Structures-Design and Thermal Structural Analysis*. Australia, University of Adelaide.